Fluorescence Probing of Solvent Accessibility and Micropolarity on Silica and Alkylated Silica Surfaces

Marcel J. Bartels,[a] Mattijs Koeberg,[a] and Jan W. Verhoeven*[a]

Keywords: Modified silica / Charge transfer fluorescence / Excimer / Solvatochromism / Maleimides

The highly solvatochromic probe "Fluoroprobe", which fluoresces in a wide range of the visible spectrum, was covalently attached to silica and alkylated silica particles to study solvent accessibility and surface micropolarity. A two step attachment method was used which was found to lead to a quite homogeneous distribution of the probes without extensive local clustering. On silica the probe experiences a local dielectric constant of $\varepsilon = 6$, while its solvent accessibility is ca. 30%. On alkylated silica this reduces to $\varepsilon = 3.4$ and ca. 23% respectively.

Introduction

In various earlier studies the surface properties of silica and alkylated silica particles, which are e.g. basic components of many chromatographic systems, have been investigated with the use of covalently attached[1−6] or strongly adsorbed[7−10] fluorescent probes. Typically, the quenching of the probe by quenchers dissolved in the surrounding solvent has been employed to gain information about the accessibility of the surface-bound probe and about the dynamics of the quencher at that surface.

In principle it is also possible to determine directly the solvent accessibility, without the use of an additional quencher, by employing a solvatochromic fluorescent probe. For this purpose the fluorogenic system Maleimidofluoroprobe (MFP), developed recently in our laboratory[11], is in principle well suited because it contains the maleimido group that allows easy attachment to various reactive sites[12][13] and because the resulting adducts show extremely solvatochromic intramolecular charge transfer fluorescence. Thus the adduct of e.g. isopropylamine and MFP was reported to undergo a shift in fluorescence wavelength from 411 nm (blue) in *n*-hexane to 666 nm (red) in acetonitrile.

This behaviour is identical to that of the parent system Fluoroprobe (FP) for which it was established that excitation leads to a strongly fluorescent intramolecular charge transfer state in which essentially one electron has been transferred from the aniline donor unit to the cyanonaphthalene acceptor unit[14−16]. Solvation of this dipolar state is responsible for the strong solvatochromism of the fluorescence emerging upon charge recombination.

[a] Laboratory of Organic Chemistry, IMC, University of Amsterdam
Nieuwe Achtergracht 129, 1018 WS Amsterdam,
The Netherlands
Fax: (internat.) +31-20/ 525-5670
E-mail: jwv@org.chem.uva.nl

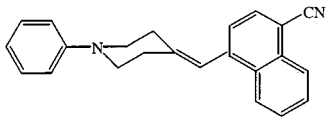

Fluoroprobe (FP)

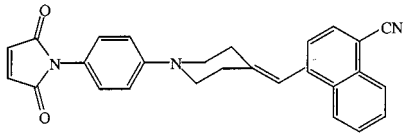

Maleimidofluoroprobe (MFP)

Scheme 1. Structures of FP and MFP

Results and Discussion

Covalent Attachment of Fluoroprobe on Silica and Alkylated Silica

A typical chromatography grade silica (Acros, particle diameter 0.035−0.07 mm) was surface-functionalized with the Fluoroprobe (FP) label at two different concentrations indicated as FP1, and FP2. This was achieved (see Scheme 2 and experimental) by first functionalising the silica with (3-aminopropyl)trimethoxysilane followed by reaction with MFP.

As can be seen from the analytical data compiled in Table 1, the amount of probe introduced in FP2 is about ten times that in FP1. This implies that at least in the latter many reactive sites for further derivatisation are still available. This is substantiated by the fact that reaction of a batch of FP1 with an excess of octadecyltrichlorosilane (see Experimental Section) allowed us to obtain a silica (RFP1) in which extensive alkylation has taken place without removing the FP probes. The extensive alkylation of RFP1 is not only evident from the analytical data compiled in Table 1

  1434−193X/99/0909−2391 $ 17.50+.50/0

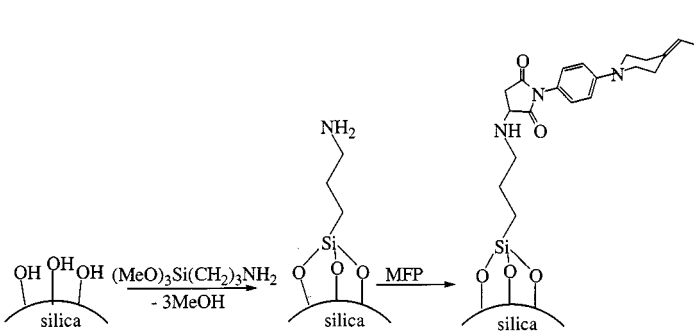

Scheme 2. General procedure for the attachment of the probe to the silica surface

but also from the very hydrophobic nature of these particles that − in contrast to FP1 and FP2 − float on water.

It should be noted that we have determined the surface area of all modified silica′s separately by mercury porosimetry (see Experimental Section). As evident from Table 1 this is quite important because it turns out that the chemical treatment has a significant influence on that surface area (see Table 1).

Table 1. Analytical data for MFP modified silica′s and surface coverage calculated therefrom (see Experimental Section)

	FP1	FP2	RFP1
probe concentration from C content (weight%)	2.7	26	8.8 (R)
probe concentration from N content (weight%)	2.8	29	1.4 (FP)
average probe concentration (mmol of probes per gram)	0.055	0.475	0.349 (R) 0.031 (FP)
Surface area (m^2 per gram)	157	80	50
Average surface area available per probe ($Å^2$)	475	14	38 (R) 270 (FP)

Since FP itself is nearly colorless we were surprised to find that FP2 displays a strong yellow color. From the diffuse reflection spectra (see Figure 1) it is evident that this yellow color is related to an absorption band with a maximum in the visible (ca. 450 nm) that cannot be accounted for by the well documented absorption properties of the isolated FP system[14][16]. We think that the most likely explanation for this phenomenon is the occurrence of intermolecular ground state charge-transfer interaction in FP2 between the donor of one and the acceptor of another, adjacent FP system. This is not unexpected because as can be seen from the data in Table 1 the FP units in FP2 must be quite closely packed with an average of one probe on 14 $Å^2$. We will return to this problem below, where we use another probe (pyrene) to study surface aggregation.

Solvent Accessibility and Local Polarity Effects for Surface-Bound Fluoroprobe on Silica and Alkylated Silica

Because of the evident interprobe effects in FP2 we will not use the fluorescence data of this sample in the following discussion on solvent accessibility and local polarity. It should be noted, however, that in contrast to their absorption spectra FP1 and FP2 displayed similar fluorescence spectra. This is probably because fluorescence only derives from isolated FP sites while sites at which two or more FP units interact to modify the absorption spectrum are non-fluorescent.

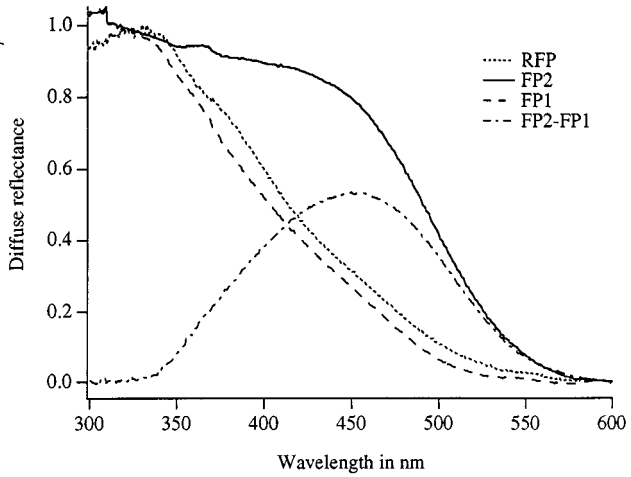

Figure 1. Diffuse reflectance spectra of FP1, FP2, and RFP1 as well as the difference spectrum FP2-FP1

Table 2. Fluorescence data for FP, FP1, and RFP1 in various solvents

	Δf	ε	FP λ_{max} in nm	FP1 λ_{max} in nm	RFP1 λ_{max} in nm
n-hexane	0.092	1.88	407	498	470
cyclohexane	0.100	2.02	410	500	
trans-decalin	0.110	2.17		496	
benzene	0.116	2.28		508	
di-*n*-pentyl ether	0.171	2.77			474
di-*n*-butyl ether	0.194	3.10	465		
ddiisopropyl ether	0.237	3.88	490		
diethyl ether	0.251	4.20	513	544	488
ethyl acetate	0.292	6.02	571	550	
tetrahydrofuran	0.308	7.58	571	560	
dichloromethane	0.319	8.93	578		502
acetonitrile	0.393	37.50	694	596	516
water	0.405	78.39		586	480[a]

[a] Floats on water.

Fluorescence maxima of FP, FP1, and RFP1 in a range of solvents are compiled in Table 2. In this table solvents are arranged according to increasing solvent polarity as expressed by the polarity parameter Δf, which is defined[17] in terms of the dielectric constant ε and the refractive index n as: $\Delta f = (\varepsilon - 1)/(2\varepsilon + 1) - (n^2 - 1)/(4n^2 + 2)$.

In all cases the fluorescence undergoes a significant red shift upon increasing solvent polarity. We now compare the solvatochromic behaviour of FP1 and RFP1 with that of Fluoroprobe (FP) itself. It has been found that the fluorescent wavelength of the latter is not significantly influenced by the presence of the succinimide bridge that arises upon coupling of MFP to an amine and therefore FP itself provides a convenient model for the behaviour of this flu-

orophore in a homogeneous solvent. Comparison between FP, FP1, and RFP1 is made by plotting (see Figure 2) the position of the fluorescence maximum (ν in cm^{-1}) as a function of the solvent parameter Δf[18−21]. The so called Lippert−Mataga (LM) plots thus obtained are linear, indicating that the dipole moment of the emissive state is solvent independent. This is as expected for the conformationally well defined FP fluorophore, for which it has been firmly established[14][22] that the emissive state has a dipole moment which is 27 ± 2 Debije larger than that of the ground state.

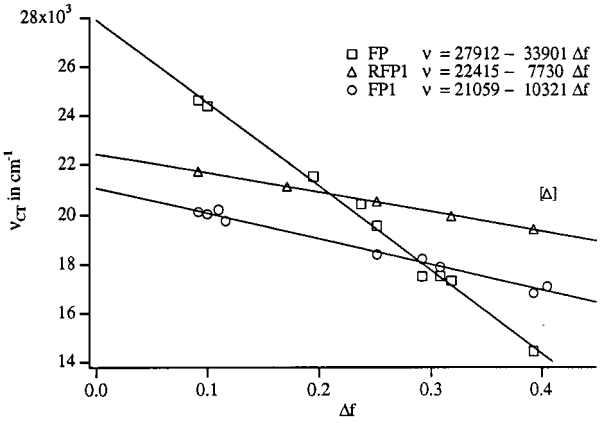

Figure 2. Lippert−Mataga plots for Fluoroprobe (FP) in a series of solvents and the modified silica′s FP1 and RFP1 dipersed in these solvents. The data point for RFP1 in water is indicated in brackets and was not used in the calculation of the regression line.

The Lippert−Mataga Equation (1) underlying the plots in Figure 2 has been derived for a point dipole (μ, in Debije) occupying a spherical cavity with radius ρ (in Å) in a continuous dielectric medium. In Equation (1) ν_0 is the fluorescence maximum (in cm^{-1}) for the gasphase isolated molecule.

$$\upsilon = \upsilon_0 - 10068(\mu^2/\rho^3)\Delta f \qquad (1)$$

Equation (1) can thus be applied to describe the behaviour of FP in a homogeneous solvent, but for FP1 and RFP1 it should be modified to take into account that only part of the solvation shell around the FP fluorophore can be occupied by the solvent while the rest is apparently occupied by the silica or alkylated silica matrix (in FP1 and RFP1, resp.). Under the assumption of additivity Equation (1) can then be modified to Equation (2), in which p is the fraction of the solvation shell accessible to the solvent and Δf_M is the effective polarity of the matrix that occupies the rest of the solvation shell.

$$\upsilon = \upsilon_0 - 10068(\mu^2/\rho^3)[p\,\Delta f + (1\text{-}p)\,\Delta f_M] \qquad (2)$$

Equation (2) implies that the solvent accessibility, as measured by p, of the FP probes in FP1 and RFP1 can directly be derived from the ratio of the slopes of the LM plots obtained for FP itself and each of these modified silica′s and that this accessibility must be greatly reduced to explain the much smaller slopes of the LM plots for FP1 and RFP1 as compared to FP.

Thus we find for FP1 p = 10321/33901 = 0.30 and for RFP1 p = 7730/33901 = 0.23.

It is interesting to note that already in FP1 the solvent accessibility seems to be less than p = 0.5, the value one would expect for a probe on a flat surface. This suggests that part of the probes in FP1 is bound in recessed locations (pores, valleys). The further decrease of the solvent accessibility in RFP1 is of course in line with expectation and substantiates the high surface coverage of the silica with alkyl chains that was calculated from the analytical data for RFP1 (see Table 1).

Another interesting parameter that can be derived from the plots in Figure 2 via application of Equations (1) and (2) is the effective polarity of the silica matrix, Δf_M. Evidently $\Delta f \equiv \Delta f_M$ at the crossing point of the LM plot for a modified silica with that for FP. From this we find that Δf_M = 0.29 for FP1 and Δf_M = 0.21 for RFP1. This corresponds e.g. closely to the Δf values for the solvents ethyl acetate (Δf = 0.292) and di-*n*-propyl ether (Δf = 0.213) which have a dielectric constant of ε = 6.02 and ε = 3.39, respectively. The latter is rather close to that of saturated alkanes ($\varepsilon \approx 2$) and testifies the significant shielding of the FP probes by the alkane chains in RFP1. In this connection it is interesting to note that for RFP1 (but not for FP1) water is a clear outlyer in the LM plot (see Figure 2) with a fluorescence maximum corresponding to a solvent of much lower polarity. This shows that the accessibility of the FP probe in RFP1 is much lower for water than for the other solvents for which it has a constant value of about 23% as estimated from the slope of the LM plot (see above). As already mentioned earlier this is also evident from the low wettability of the RFP1 particles that actually float on water.

Probe Distribution as a Function of the Degree of Surface Loading

As mentioned in the preceding section the probe concentration in FP1 and RFP1 was kept rather low because at higher loading in e.g. FP2 indications for strong inter-probe interaction were obtained from the diffuse reflectance spectrum (see Figure 1).

In order to obtain more information about the probe distribution, resulting from the present method of attachment, we prepared a number of samples in which the same surface-probe linking method is employed that was used for FP1 and FP2 (see Scheme 2), but in which the reagent MFP in the last step was substituted by the also fluorogenic reagent *N*-(1-pyrenyl)maleimide.

This provided the samples P1, P2, and P3 with increasing surface loading of a fluorescent pyrene unit. The well-known strong tendency of these units to form a fluorescent excimer[23] can now be employed to detect via fluorescence spectroscopy the presence of probes that are within close range.

In Table 3 analytical data for the P1, P2, and P3 samples are given as well as the inverse surface density (Å^2 per probe) calculated therefrom. The area that a pyrene unit can occupy varies between ca. 30 and ca. 100 Å^2 in respectively a perpendicular and a parallel orientation. It is thus clear that while they must be closely packed in P3, in P2 and especially in P1 most of the pyrenes should have a quite large distance from each other preventing excimer formation provided that they are statistically distributed.

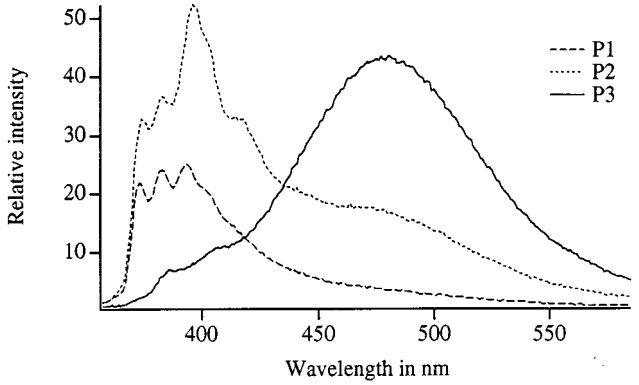

Figure 3. Fluorescence spectra of P1, P2, and P3 in cyclohexane (spectra were obtained by excitation at 320 nm)

The fluorescence spectra of P1, P2, and P3 in cyclohexane are displayed in Figure 3. As predicted, the structured monomer fluorescence of pyrene is dominant in P1 while in P3 this is almost completely quenched and substituted by the red-shifted and structureless excimer fluorescence at 480 nm. The situation in P2 is intermediate with both excimer and monomer fluorescence clearly present.

It should be noted that pyrene has extensively been used as a luminescent probe on silica. In at least one case it was noted that covalent attachment leads to modified silica′s in which the probes tend to be clustered predominantly into regions of high density. However, in that case the reagent molecules that react with the silica already contain the pyrene units[2], which might induce such clustering via their π-π interaction. In our case (see Scheme 2) a two-step procedure is used, which could avoid this, and was therefore expected to lead to a more homogeneous probe distribution.

In order to analyse this in more detail we note that for a statistical distribution the fraction of pyrenes that can form excimers can be approximated as $E = 1/2(\pi NR^2)$ in which N is the number of pyrenes per unit area and R is the maximum centre to centre distance at which excimer formation still occurs. If so, the intensity ratio of monomer and excimer fluorescence (I_M/I_E) is given by Equation (3):

$$I_M/I_E = [2/(\pi NR^2) - 1]\Phi_M/\Phi_E \quad (3)$$

In Equation (3) Φ_E/Φ_M is the ratio of the excimer and monomer fluorescence quantum yields.

In Figure 4 we now plot for P1, P2, and P3 as a function of $1/N$ (i.e. the area available per probe) the fluorescence intensity ratios at 375 nm and 500 nm where the fluorescence is dominated by monomer and excimer respectively. From the regression a value of $R = 3.7$ Å is calculated. This is a very acceptable value for excimer formation between two aromatic species[2][23] and together with the linearity of the plot obtained therefore strongly indicates that our two-step covalent linking scheme leads to a fairly statistical distribution of probes over the available surface area.

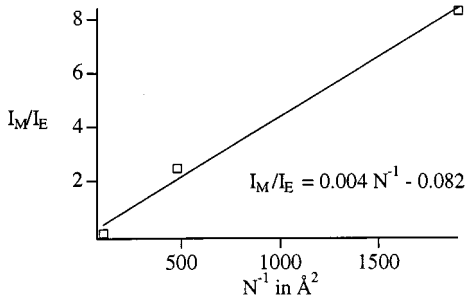

Figure 4. Ratio of monomer (at 375 nm) and excimer fluorescence (at 500 nm) for P1, P2, and P3 as a function of the area available per probe

Table 3. Analytical data for pyrene modified silica′s and surface coverage calculated therefrom (see Experimental Section)

	P1	P2	P3
probe concentration from C content (weight%)	0.06	0.4	4.2
probe concentration from N content (weight%)	–	0.1	2.8
average probe concentration (mmol of probes per gram)	0.0016	0.0079	0.11
Surface area (m^2 per gram)	18	30	67
Average surface area available per probe (Å^2)	1908	480	102

As noted by one of the referees the average area available to each probe molecule is very similar in FP1 (475 Å^2, see Table 1) and in P2 (480 Å^2, see Table 3). In the latter system some inter-probe interaction is detectable from the contribution of excimer emission (see Figure 3) and because of the similar probe sizes it is thus feasible that some inter-probe interaction could also occur in FP1. That this is not evident from the spectroscopic data of FP1 must be due to the fact that (in contrast to P2) it does not lead to a new emission band but only causes some quenching of the intramolecular CT fluorescence of those FP fluorophores that happen to be in direct contact. Inter-probe interaction was evident from the absorption data of FP2 as discussed above, but this is of course a much less sensitive tool than fluorescence and requires a much higher fraction of the probes to be involved

Experimental Section

UV-Vis reflectance measurements were recorded on a Cary 3E spectrophotometer using an integrating sphere attachment. Fluorescence spectra were recorded on Spex Fluorolog II and Spex Fluorolog III spectrofluorometers.

For elemental analysis measurements a Vario EL was used. Both carbon and nitrogen mass fractions were measured for all samples.

For FP1 and FP2 these values were divided by the mass fractions of the specific atom in the probe, including the silane amine spacer (0.714 for C and 0.111 for N), to obtain the mass fraction of the probe. For P1, P2, and P3 the same calculations were used, the mass fraction C and N of these probes is 0.719 and 0.073, respectively. For RFP1 the measured nitrogen mass fraction was used to calculate the mass fraction FP probes. This was then used to correct the C content for the FP contribution, thus giving the alkyl chain loading as the difference.

Surface areas were determined by mercury porosimetry[24][25], on a Pascal 440 of CE instruments (DIN 66133 procedure), assuming cylindrically shaped pores. With a penetrometer the decrease in volume (dV in m^3), was measured while the pressure (p in Pa) increases until a plateau was reached. The maximum pressure used was 400 MPa. The specific Brunauer−Emmett−Teller surface A (in square meters per gram silica)[26], was then calculated via Equation (4) in which m is the mass of the sample (in g), Θ is the contact angle between the mercury and the probe surface (130° at 25°C). The surface free energy of liquid mercury is given by γ_L (0.48 Jm^{-2}).

$$A = \frac{-1}{m \cdot \gamma_L \cdot \cos\Theta} \cdot \int_0^{V_{max}} p \cdot dV \qquad (4)$$

The synthesis of maleimidofluoroprobe (MFP) has been described before by Verhey et al.[11] *N*-(1-pyrenyl)maleimide was purchased from Fluka (> 99%). The silica gel, purchased from Acros (d = 0.035−0.07 mm, pore 6 nm), was activated by stirring it in an aqueous solution of KOH (pH 12) for one hour. The activated silica particles were washed with water and ethanol and dried overnight at 100°C. To connect the probe molecules to the silica surface a silane−amine linker was first introduced[6][27]. For this purpose (3-aminopropyl)trimethoxysilane from Fluka (> 97%) was used without further purification. For FP1 and FP2 the silica gel and the appropriate amount of silane reactant in toluene (30 mL) were refluxed for 1.5 hour. Purification was done by washing the product on a glass filter with toluene, methanol, and benzene. This reactively modified silica was subsequently put in a solution of MFP in toluene (30 mL). After stirring for 3 hours at 40°C the final product was obtained. Depending on the MFP concentration the color of the product was yellow to pale yellow. At last the products were washed with toluene, methanol and benzene. For FP1 and FP2 respectively 0.46 g and 0.46 g silica gel, 10 μL (57 μmol) and 0.24 mL (1.4 mmol) (3-aminopropyl)trimethoxysilane and 31 mg (75 μmol) and 0.22 g (0.54 mmol) MFP were used.

The first part of the synthesis of RFP1 was identical to the synthesis of FP1. Here we used 0.30 g silica gel, 2.9 μL (16 μmol) (3-aminopropyl)trimethoxysilane and 9.6 mg (24 μmol) MFP. After this the modified silica gel was stirred in toluene (20 mL) at 90°C for 2 hours under the addition of 0.39 mL (1.0 mmol) octadecyltrichlorosilane (Acros, 95%), followed by washing with toluene, methanol, and benzene. The final product floated on water.

The synthesis of P1, P2, and P3 were performed in the same way and under the same conditions as the synthesis of FP1 and FP2. For P1, P2, and P3 0.49 g, 0.46 g, and 0.44 g silica gel, 0.30 mL (1.6 mmol), 1.0 mL (5.7 mmol), and 10 mL (57 mmol) (3-aminopropyl)trimethoxysilane and 1 mg (3.4 mmol), 3 mg (10 mmol), and 18 mg (61 mmol) *N*-(1-pyrenyl)maleimide were used, respectively.

Acknowledgments

Marjo C. Mittelmeyer-Hazeleger is gratefully acknowledged for performing the mercury porosimetry measurements and Jan Dijkink for executing the elemental analyses. This research has been financially supported by the Council for Chemical Sciences of the Netherlands Organization for Scientific Research (CW-NWO).

[1] C. H. Lochmüller, D. B. Marshall, D. R. Wilder, *Anal.Chim. Acta* **1981**, *130*, 31.
[2] C. H. Lochmüller, A. S. Colborn, M. L. Hunnicutt, J. M. Harris, *J. Am. Chem. Soc.* **1984**, *106*, 4077.
[3] C. H. Lochmüller, M. L. Hunnicutt, *J. Phys. Chem.* **1986**, *90*, 4318.
[4] A. L. Wong, J. M. Harris, *J. Phys. Chem.* **1991**, *95*, 5895.
[5] A. L. Wong, M. L. Hunnicutt, J. M. Harris, *Anal. Chem.* **1991**, *63*, 1076.
[6] M. Ayadim, J. L. Habib, A. P. de Silva, J. P. Soumillion, *Tetrahedron Lett.* **1996**, *37*, 7039.
[7] M. A. T. Marro, J. K. Thomas, *J. Photochem. Photobiol. A: Chem.* **1993**, *72*, 251.
[8] R. K. Bauer, P. de Mayo, W. R. Ware, K. C. Wu, *J. Phys. Chem.* **1982**, *86*, 3781.
[9] R. K. Bauer, P. de Mayo, L. V. Natarajan, W. R. Ware, *Can. J. Chem.* **1983**, *62*, 1279.
[10] L. D. Weis, T. R. Evans, P. A. Leermakers, *J. Am. Chem. Soc.* **1968**, *90*, 6109.
[11] H. J. Verhey, C. H. W. Becker, J. W. Verhoeven, J. W. Hofstraat, *New J. Chem* **1996**, *20*, 809.
[12] H. J. Verhey, L. G. J. van der Ven, C. H. W. Bekker, J. W. Hofstraat, J. W. Verhoeven, *Polymer* **1997**, *38*, 4491.
[13] J. M. Warman, R. D. Abelon, H. J. Verhey, J. W. Verhoeven, J. W. Hofstraat, *J. Phys. Chem. B* **1997**, *25*, 4913.
[14] G. F. Mes, B. de Jong, H. J. van Ramesdonk, J. W. Verhoeven, J. M. Warman, M. P. de Haas, L. E. W. Horsman-van den Dool, *J. Am. Chem. Soc.* **1984**, *106*, 6524.
[15] T. Scherer, W. Hielkema, B. Krijnen, R. M. Hermant, C. Eijckelhoff, F. Kerkhof, A. K. F. Ng, R. Verleg, E. B. van der Tol, A. M. Brouwer, J. W. Verhoeven, *Recl. Trav. Chim. Pays-Bas* **1993**, *112*, 535.
[16] R. M. Hermant, N. A. C. Bakker, T. Scherer, B. Krijnen, J. W. Verhoeven, *J. Am. Chem. Soc.* **1990**, *112*, 1214.
[17] H. Knibbe, *Charge-transfer complex formation in the excited state*. PhD thesis, Free University of Amsterdam, **1969**.
[18] E. Lippert, *Z. Naturforsch* **1955**, *10A*, 541.
[19] E. Lippert, *Z. Electrochem.* **1957**, *61*, 962.
[20] N. Mataga, Y. Kaifu, M. Koizumi, *Bull. Chem. Soc. Jpn.* **1955**, *28*, 690.
[21] N. Mataga, Y. Kaifu, M. Koizumi, *Bull. Chem. Soc. Jpn.* **1956**, *29*, 465.
[22] S. V. Rodrigues, A. K. Maiti, H. Reis, W. Baumann, *Mol. Phys.* **1992**, *75*, 953.
[23] T. Förster. In: *The Exciplex* (Eds.: M. Gordon, W. R. Ware), Academic Press Inc., **1975**, 1.
[24] H. M. Rootare, C. F. Prenzlow, *J. Phys. Chem.* **1967**, *71*, 2733.
[25] K. Unger, E. Schadow, H. Fischer, *Z. Phys. Chem. N. F.* **1976**, *99*, 245.
[26] S. Brunauer, P. H. Emmett, E. Teller, *J. Am. Chem. Soc.* **1938**, *60*, 309.
[27] A. Cauvel, G. Renard, D. Brunel, *J. Org. Chem.* **1997**, *62*, 749.
Received December 23, 1998
[O98594]